On Osmotic Heat Powered Cycles Driven by Thermal Saturation-Precipitation of Aqueous Solutions*

The basis of a novel concept for osmotic heat powered cycles driven by the thermal dependence of the solubility of aqueous solutions inducing the continuous thermal precipitation/dissolution of solute is outlined. In this osmotic concept, given an aqueous solution with a temperature near to its temperature of saturation, if an external thermal input is applied (either by heating or cooling the solution depending of the specific thermal dependence of the solubility) then, partial precipitation of the solute takes place. By separating the solute precipitate from the remaining depleted solution -generally referred as supernatant, and restoring its initial temperature, the net result is the conversion and storing of thermal energy into osmotic energy contained in two streams with different salinities which can be released only when both streams are deliberately mixed by using a semi-permeable membrane. Utilizing a simplified physical model, a first estimation for the the maximum extractable energy per unit of volume of solution was calculated. The specific cases for some common salts were compared. Additional R&D is required in order to arrive at a reliable practical and commercial design.

Keywords. *Thermal solubility of aqueous solutions; Osmotic heat engines; Pressure-retarded osmosis, (PRO); Salinity power, Renewable energy.*

1. Introduction

The possibility to extract energy from salinity gradients has been investigated at least from the second half of the last century. Back to the 1950s, Pattle, [1] was perhaps the first to mention the untapped source of power obtainable when a river mixes with the sea, and in the 1970s, the first method and apparatus for generating power was presented, [2], [3]. Since then, and motivated specially by the growing interest for the use of clean renewable energy sources in the last decades, harnessing the energy released during the spontaneous mixing of two solutions of different salinities has shown an important revival and several research aspects such as real performance [4]; thermodynamic efficiencies [5]; practical limit of energy production [6]; membrane technology [7], [8]; and designs [9], has been addressed. Among the applications offered by the technology one of the most interesting prospects is the possibility to run heat powered cycles.

Osmotic heat powered cycles or also called as osmotic heat engines (OHEs) are heat cycles in which an engine is harnessing salinity gradients as source of energy generation. Although there are different techniques to run such engines with continuous concentration gradient flow [10],[11] as well as designs [12], however, all of them are based in collect low grade thermal energy to concentrate a salt solution, which can be performed by, for example, vaporization, and then releasing continuously the chemical potential energy by using semipermeable membrane allowing the solvent to pass to the concentrated solution side by osmosis and then creating an hydraulic pressure to run, say, a turbine,[13]. Therefore, the main disadvantage of those heat engines is the poor efficiency limited by the high heat of vaporization of the working fluid needed for re-concentrate the draw solution, [14].

The object of the present work was to analyze a different approach based in the thermal dependence of the solubility featured by aqueous solutions. Here, it will be shown that by the proper choice of the concentration of a given common aqueous solution an osmotic heat engine can be driven by alternating solute precipitation and mixing when heat is either applied (by heating the solution) or extracted (by cooling the solution) depending of the thermal behavior of the solubility of the solution.

2. Materials and Methods

2.1 Statement of the core idea

Consider the thermal cycle depicted in Fig. 1, where for the sake of argument it was chosen a solution which increases its solubility with the temperature but the concept is equally valid for solutions featuring the opposite behavior, i.e., decreasing its solubility with temperature as is shown in Fig. 2. The meaning of the various terms in Fig. 1 are defined in the nomenclature.

To begin with, fix the given aqueous solution with an initial temperature, say, T_2 and concentration C_o -which is just below its saturation concentration at that temperature (i.e., below of S_2 as depicted in Fig. 1). Therefore, initially the aqueous solution is in an *"undersaturated"* state.

Now, if a thermal shift occurs and temperature decrease from T_2 to T_1 and crossing the line of solubility, then the initial concentration C_o is now higher than the

*Corresponding author: Tel.: +32 14 33 21 94; Electronic address: francisco.javier.arias@upc.edu

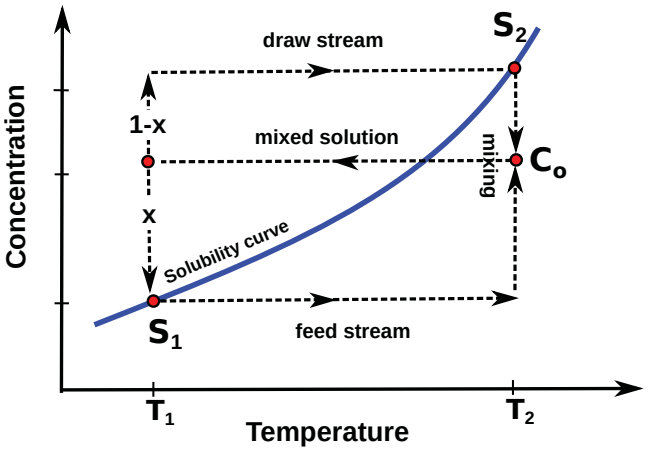

FIG. 1: The basis of the proposed osmotic heat engine driven by the precipitation of saturated aqueous solutions.

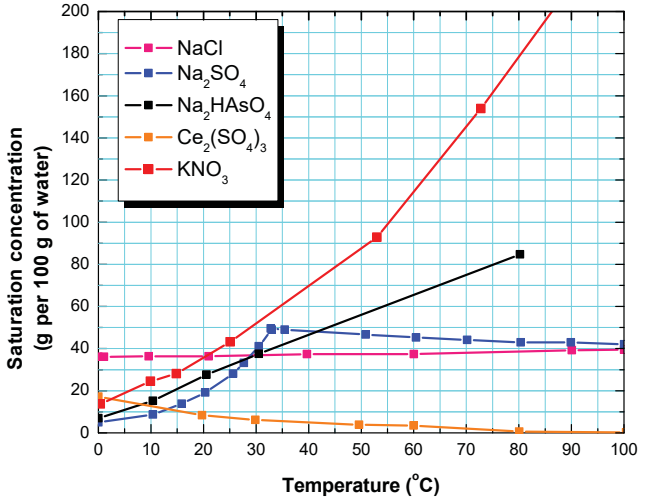

FIG. 2: Solubility vs. temperature for a variety of salts. Data are taken from [16]. Particulary interesting is KNO_3 because the strong dependency of the solubility with temperature as well as the broad range of temperature allowed.

saturation concentration S_1 at T_1, and then the initial unsaturated solution is now in a *"supersaturated"* state and as a result precipitation takes place and a certain fraction of dissolved solute precipitate. Therefore, one requirement to run this osmotic heat cycle is that the initial concentration of the aqueous solution be undersaturated at its initial temperature and supersaturated at the final temperature, i.e., satisfying

$$S_2 > C_o > S_1 \tag{1}$$

Once supersaturation occurs, the excess of solute precipitate and can be easily separated by using a proper filter. At this point, we have on one hand a homogeneous solution which has been depleted of solute - generally referred as supernatant, and on the other hand a heterogeneous solution containing the precipitate solute.

Now referring to Fig. 1, if the total volume of the solution is separated into two volumes one with a volume fraction (x) containing the depleted supernatant with the concentration S_1 which is actually the maximum concentration allowed at T_1, and another volume with fraction $(1-x)$ containing the suspended solute precipitate, and if both volumes are heated until recovering the initial temperature T_2, then the suspended heterogeneous solute contained in the volume of fraction $(1-x)$ is totally dissolved forming a homogeneous solution. If the proper fraction (x) was chosen it is possible that the dissolved solute in the fraction $(1-x)$ get the maximum saturation concentration at T_2, i.e., S_2 and then maximizing the gradient of salinity between both streams which is desired for extractable osmotic energy upon mixing.

This rather simple, robust and inexpensive thermal process could find several applications, for example, in solar thermal energy as is illustrated in Fig. 3, or even as a new kind for long thermal storage energy if one considers that the osmotic energy can be stored indefinitely and only released when deliberately both streams are put together and then eliminating the limited storage provided by sensible or latent heat systems which unavoidably loss energy with the environment or require additional insulation systems.

As regard the operation of the osmotic engine, this will operate as a traditional pressure-retarded osmosis (PRO) process, with the only exception that a *precipitator-module* will be required. In traditional OHEs, the high concentration draw solution and the low concentration feed stream are pumped into the opposite side of the membrane module by the add of a pressure exchanger (PEX) which basically transform the osmotic energy released by the mixing into an effective hydraulic pressure gradient which propels the fluid in the system. By the use of a turbine this flow can be used to generate power, [15].

As mentioned before, the only difference with the traditional OHEs, is the need for a *precipitator-module* with the purpose of continuous separation of the heterogeneous suspended solute from the supernatant. However, because the expected Stokes number **Stk** is extremely low, the precipitator module can removes the suspended solute in a continuous and simple way as depicted in Fig. 4 and also by the same motive sedimentation at the bottom of the vessel doesn't occur. Indeed, the Stokes number is defined as

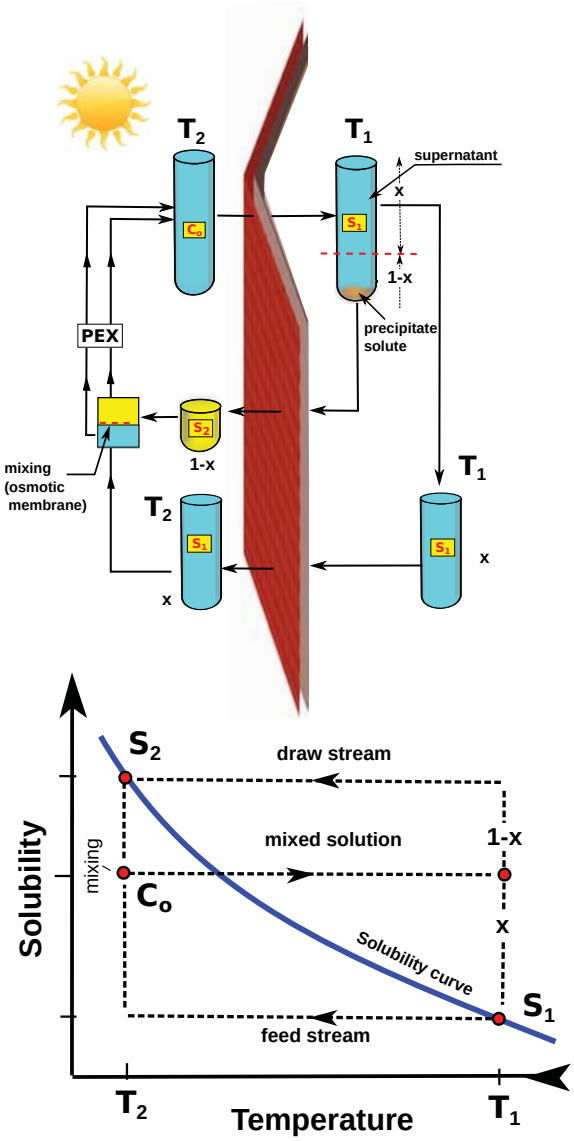

FIG. 3: Sketch for a possible osmotic heat engine driven by solar thermal energy.

$$\mathbf{Stk} = \frac{\rho_p d_p^2 u_o}{18 \mu l_o} \tag{2}$$

where ρ_p is the solute particle density, d_p is the solute particle diameter, μ the liquid dynamic viscosity, u_o is the fluid velocity ad l_o the characteristic dimension of the system. Very small Stokes number means that particles will follow the fluid streamlines closely, which translate into the possibility that particles can be remove just by interposing a filter and bifurcating the main stream, as depicted in Fig. 4. It is easy to see, that with $\rho_p \approx 10^3$ kg/m^3; $d_p \approx 1\mu$ m; $u_o \approx 10^{-2}$ m; $\mu \approx 10^{-3}$ Pa.s; and $l_o \approx 1$ m, this possibility for the precipitator is valid.

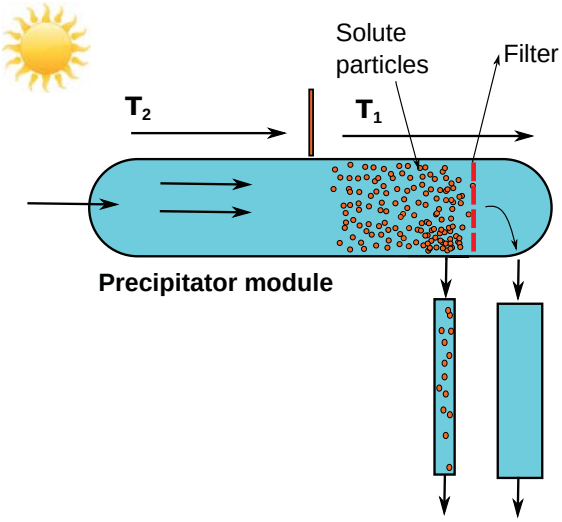

FIG. 4: Precipitator module for continuous removal of suspended solute. Owing to the small Stokes number solute particles will follow closely stream lines and then sedimentation at the bottom of the vessel doesn't occur.

2.2 Extractable energy

Bearing the above simplified scheme in mind, we can proceed with some theoretical treatment.

First of all, it is necessary to calculate the required volume fraction (x) which allows the mentioned cycle. This calculation may be easily found by a balance of mass of the solute before and after the precipitation takes place as

$$C_o = S_1 x + S_2(1-x) \tag{3}$$

and then the volume fraction of the feed given by

$$x = \frac{S_2 - C_o}{S_2 - S_1} \tag{4}$$

where the mixed solution C_o must satisfy the relationship given by Eq.(1), i.e., $S_2 > C_o > S_1$.

The maximum energy available from the osmotic mixing may be estimated by the amount of Gibbs free energy per mole of mixed solution generated from mixing two solutions of different salinities in an isothermal and reversible process. Then, it must be considered that the next calculation reported result from an idealized process and therefore this should not be misconstrued as an attempt to typify estimates. Nonetheless, the idealized case will provide an upper limit and then will provide important guidance to analyze the concept. The amount

of Gibbs free energy per mole of mixed solution generated from mixing two solutions of different salinities in an isothermal and reversible process is given by

$$-\frac{\Delta G_{nm}}{iRT} = f_M \ln(\gamma_M f_M) - \frac{n_F}{n_M} f_F \ln(\gamma_F f_F)$$

$$-\frac{n_D}{n_M} f_D \ln(\gamma_D f_D) \quad (5)$$

where i is the vant´Hoff factor for electrolytes (e.g, $i = 3$ for Na_2SO_4; $i = 2$ for NaCl, etc...), R is the gas constant; T is absolute temperature; and f; n; and γ are the mole fraction of species, total moles of the species and activity coefficients of species , and the subscripts M; F; and D stand for the mixed, feed and draw solutions, respectively. When the solution is perfectly diluted or ideal, the activity coefficients are approximated equal to 1 and in this case the expression is simplified notoriously, [4]. However, for the present case working with concentrations near or at the saturation point the above approximation is not longer valid. The deviation of Eq.(5) from the ideal case can be calculated by considering the osmotic coefficients θ_M, θ_F and θ_D of each specie and yields .

$$\frac{\Delta G_{nm}}{iRT} = \theta_M f_M \ln(f_M) - \frac{n_F}{n_M} \theta_F f_F \ln(f_F)$$

$$-\frac{n_D}{n_M} \theta_D f_D \ln(f_D) \quad (6)$$

where the osmotic coefficient of the i-specie was defined by

$$\theta_i = \frac{\ln(\gamma_i f_i)}{\ln(f_i)} \quad (7)$$

These osmotic coefficients give the deviation of a solvent from ideal behavior and are dependent on the concentration of each species, where for an ideal (infinite dilute solution) they are equal to unit. Fig. 5 shows as an example the osmotic coefficient for $NaSO_4$, [26] and NaCl, [25] and KNO_3. If the solubility of the given solution doesn't changes appreciably with changes in temperature or the change in temperature in the cycle is not very strong, the molar concentrations c_M; c_F; c_D in the mixed, feed, and draw solutions could be not very different, and then it could be allowable to assume as first approximation that the osmotic coefficients are approximately equal, i.e., $\theta_M \approx \theta_F \approx \theta_D = \theta$. Further, if it can be considered negligible the volume of the solute to the volume of solution, the ratios of total moles in Eq.(5) can be given by the volume fractions as $\frac{n_F}{n_M} \approx \phi$; and $\frac{n_D}{n_M} \approx 1 - \phi$, and then, the change of Gibss energy of mixing per volume of total mixed solution simplifies as

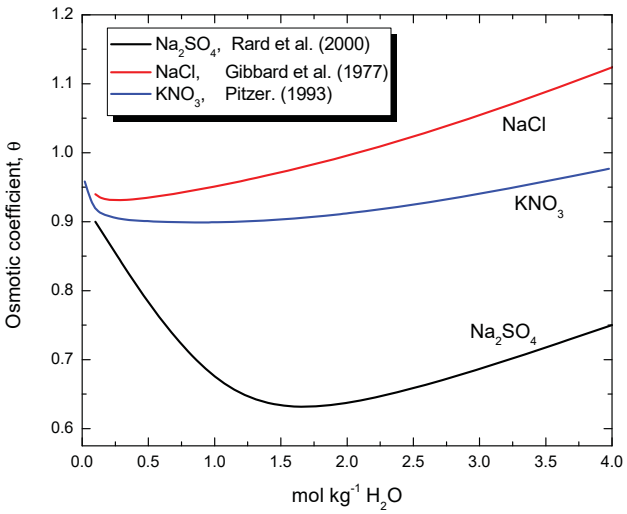

FIG. 5: Osmotic coefficient for Na_2SO_4, [25], and NaCl,[26], and KNO_3, [27], at 25^{o}C.

$$\frac{\Delta G_{vm}}{iRT} \approx \theta \left[c_M \ln(c_M) - \phi c_F \ln(c_F) - (1-\phi) c_D \ln(c_D)\right] \quad (8)$$

which after replacing $c_M = C_o$; $c_F = S_1$; $c_D = S_2$; and $\phi = x$, we obtain

$$\Delta G_{vm} \approx iRT\theta \left[C_o \ln(C_o) - xS_1 \ln(S_1) - (1-x) S_2 \ln(S_2)\right] \quad (9)$$

where x is given by Eq.(4).

3. Discussion and Results

3.1 Discussion

To obtain some idea of the extractable energy predicted by Eq.(9) , we will analyze the specific case for the aqueous solution Na_2SO_4, Na_2HAsO_4 and KNO_3 which were chosen because the strong dependence of the solubility with temperature, as is shown in Fig. 2. For Na_2SO_4 the temperature was between 278 K to 323 K, i.e., $\Delta T = 45$ K; for Na_2HAsO_4 between 288 K to 353 K, i.e., $\Delta T = 65$ K, and for KNO_3 between 282 K to 357 K. , i.e., $\Delta T = 75$ K. The resulting curves are shown in Fig. 6 for Na_2SO_4, Na_2HAsO_4 , and deserving special consideration the case for KNO_3 in Fig. 7 which due to its strong thermal dependence of solubility plus the broad temperature range allows a considerable larger amount of energy per volume of solution.

3.2 Osmotic power

One of the major aspects to be considered in the thermal osmotic system is the attainable power density per

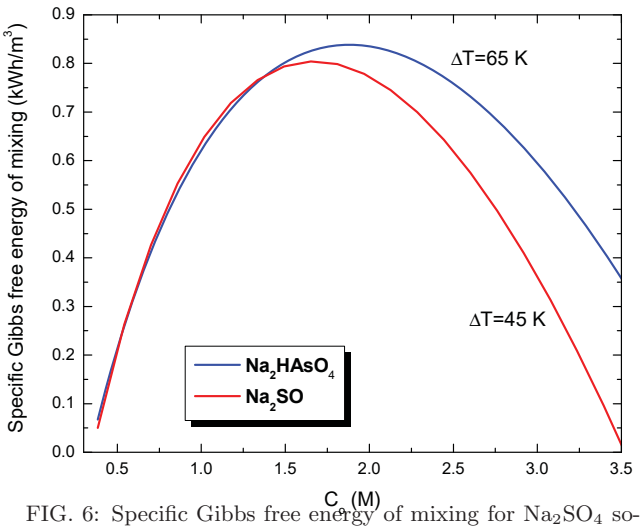

FIG. 6: Specific Gibbs free energy of mixing for Na_2SO_4 solution $\Delta T = 45$ K; and Na_2HAsO_4 with $\Delta T = 65$ K.

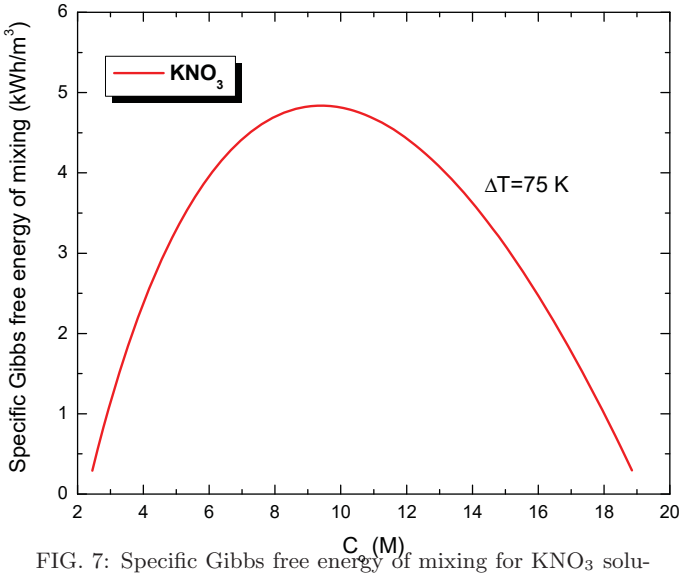

FIG. 7: Specific Gibbs free energy of mixing for KNO_3 solution $\Delta T = 75$ K.

membrane area of a module which is limited by the slow rate of media transfer through the membrane and then fixing the rate at which work can be done by the cycle. The power density per membrane area generated in the system, W_s, is approximately equal to the flow rate across the membrane Q per membrane area A_m multiplied by the hydraulic difference ΔP, i.e., $W_s \approx \frac{Q}{A_m}\Delta P$,[4]. On the other hand, the water flux across the membrane per membrane area $\frac{Q}{A_m}$ may be defined in terms of the membrane water permeability coefficient A, the osmotic pressure difference at the draw side and the feed side of the membrane , $(\pi_d - \pi_f)$, the hydraulic pressure ΔP difference across de membrane,[28]

$$\frac{Q}{A_m} = A\left[(\pi_d - \pi_f) - \Delta P\right] \tag{10}$$

and therefore the power density per membrane area of a module as

$$W_s = A\Delta P\left[(\pi_d - \pi_f) - \Delta P\right] \tag{11}$$

the value of ΔP which maximizes the power density is given when the derivative with respect ΔP is zero, which occurs when $\Delta P = \frac{(\pi_d - \pi_f)}{2}$ and then the maximized power density w_s^* given by

$$W_s^* = \frac{A(\pi_d - \pi_f)^2}{4} \tag{12}$$

or considering the expression for the osmotic pressure as function of concentration $\pi_i = iRTc_i$

$$W_s^* = A\left[\frac{RTi(S_2 - S_1)}{2}\right]^2 \tag{13}$$

In the above equation, it is easy to see that the power is maximized by maximizing the salinity gradient which is obtained by using the fraction feed (x) calculated in previous section. Finally, for many of the aqueous solutions composed by common salts the thermal dependence with solubility is almost linear (see Fig. 2), and then if it is allowable to define a coefficient of thermal solubility as Σ_s given by

$$\Delta S \approx \Sigma_s \Delta T \tag{14}$$

then Eq.(13) can be rewritten as

$$W_s^* \approx A\left[\frac{RTi\Sigma_s\Delta T}{2}\right]^2 \tag{15}$$

The above expression, give us the power of the cycle as function of the thermal gradient. It is seen that the aqueous solutions which have large coefficients of thermal solubility Σ_s and also a broad range of temperature ΔT will be able to generate more power, and because the dependence if squared $\propto (\Sigma_s\Delta T)^2$ it is imperative to use salts with large numbers for Σ_s and which allows working with a broad range of temperatures.

To obtain an idea of the power density predicted by Eq.(15) we assume a typical value of the permeability coefficient for commercial membranes $A \approx 2$ l/(hm^{2}bar). The resulting curves are shown in Fig. 6 for Na_2SO_4, and KNO_3. It is seen that for moderate thermal gradients $\Delta T \approx 30$ K, the density powers per unit membrane area could be around 40 W/m^2 to 400 W/m^2, depending of the salt used, and up to 0.2 kW/m^2 to 2 kW/m^2 for

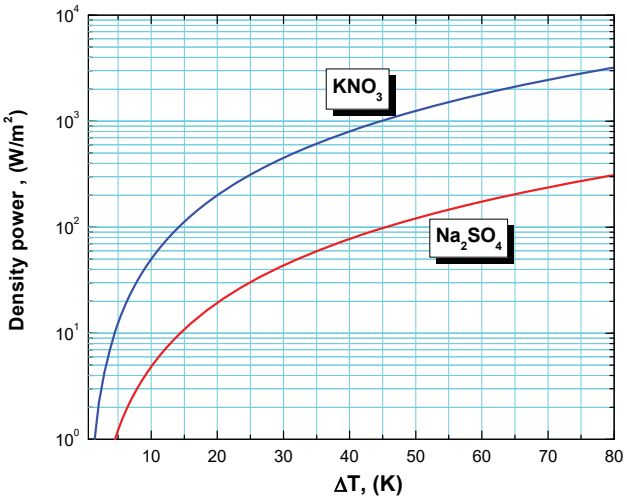

FIG. 8: Attainable power density per membrane area as function of the difference of temperature ΔT for Na_2SO_4 and KNO_3 .

$\Delta T = 70$ K.

Although the previous calculation allow us a first estimate of the achievable power by the proposed osmotic engine, however, caution must be taken. The power reported result from unavoidable idealizations required if one desires analytical expressions and are therefore not intended to typify power estimates. The efficiency of any osmotic engine is very sensitive to the membrane efficiency and performance determined mostly by the membrane water permeability coefficient which is nowadays a subject with a vigorous investigation and where significant enhancements with the use of carbon nanotubes (CNTs) are periodically reported, [29]. In addition, because the complexity of the osmotic mechanism, the water permeability coefficient could be either enhanced or lowered by working at high concentration gradients whose behavior could be also dependent of the specific salt used. Likewise, the lifetime of the membrane working in such high concentration gradients must be in future experimental studies properly addressed. As regard to the kind of salts, it seems that common and inexpensive salts can be good candidates, and it is plausible that *"designer solutions"* could be patented depicting unusual high thermal dependence of the solubility which translate into an important enhancement of the attainable power (see Fig. 2 and Fig. 8).
In summary, despite the several uncertainties raised with the proposed concept, the present study will provide important guidance in future efforts to analyze this new kind of osmotic heat engine and encourage a careful experimental investigation of the subject. Additional R&D is required in order to arrive at a reliable practical and commercial design.

4. Summary of results and conclusions

An osmotic heat engine working by the cyclic thermal precipitation and mixing of aqueous solutions close to the saturation was discussed and the theoretical basis outlined. Some interesting conclusions result from this preliminary work as follows:

(a) Thermal dependence of solubility of aqueous solutions can be used to run an osmotic heat powered cycle by the proper choice of the concentration of the aqueous solution.

(b) It is seen that for moderate thermal gradients $\Delta T \approx 30$ K, the density powers per unit membrane area could be around 40 W/m^2 to 400 W/m^2, depending of the salt used, and up to 0.2 kW/m^2 to 2 kW/m^2 for $\Delta T = 70$ K.

(c) Additional R&D is required in order to arrive at a reliable practical and commercial design.

Nomenclature

A = permeability coefficient of the membrane
A_m = area of the membrane
c = concentration
d_p = diameter of solute particle
f = mole fraction of species
ΔG = free Gibbs energy per unit volume of solution
i = the vant´Hoff factor for electrolytes
Δn_m = number of moles precipitated per volume
ΔP = hydraulic pressure
Q = flow rate across the membrane
R = ideal gas constant
S = saturated concentration
Stk = Stokes number
ΔT = difference temperature
T = temperature
V = volume
x = volume fraction of the low-concentration solution (feed)

Greek symbols

ρ = density of the solvent
ρ_p = density of the solute
$\bar{\rho}$ = equivalent density of the solution
μ = dynamic viscosity
π = osmotic pressure
θ = osmotic coefficient
Σ_s = solubility thermal coefficient defined by Eq.(**??**)
γ = activity coefficient

subscripts symbols

o = initial, reference
1 = low salinity concentration, low temperature
2 = high salinity concentration, high temperature
D = high salinity concentration (draw)

F = low salinity concentration (feed)
M = mixture
p = solute particle

Acknowledgements

This research was supported by the Spanish Ministry of Economy and Competitiveness under fellowship grant Ramon y Cajal: RYC-2013-13459.

References

[1] Pattle RE. 1954. Production of electric power by mixing fresh and salt water in the hydroelectric pile. Nature. 174 (4431). http://dx.doi.org/10.1038/174660a0
[2] Loeb S, Norman RS. 1975. Osmotic power plants. Science. 189: 654-655, http://10.1126/science.189.4203.654
[3] Loeb S. Method and apparatus for generating power utilizing pressure retarded-osmosis, US Patent 4,193,267, Ben-Gurion University of the Negev Research and Development Authority, Beersheba, Israel, US (1980).
[4] Yip NY, Elimelech M. Performance limiting effects in power generation from salinity gradients by pressure retarded osmosis. Environ. Sci. Technol 2011; 45: 10273-10282, http://10.1021/es203197e
[5] Yip NY, Elimelech M. Thermodynamic and energy efficiency analysis of power generation from natural salinity gradients by pressure retarded osmosis Environ. Sci. Technol 2012; 46: 5230-5239, http://10.1021/es300060m
[6] Minseok Kim, Suhan Kim. 2018. Practical limit of energy production from seawater by full-scale pressure retarded osmosis. Energy, Volume 158, 1, p.p 373-382
[7] Han G, Zhang S, Li X, Chung TS. 2015. Progress in pressure retarded osmosis (PRO) membranes for osmotic power generation. Progress in Polymer Science; 51: 1-27. http://10.1016/j.progpolymsci.2015.04.005
[8] Yingxue Chen, Ranjan Vepa, Mohammad Hasan Shaheed. 2018. Enhanced and speedy energy extraction from a scaled-up pressure retarded osmosis process with a whale optimization based maximum power point tracking. Energy, Volume 153, 15, p.p 618-627.
[9] Klaysom C, Cath TY, Depuydt T, Vankelecom IFJ. 2013. Forward and pressure retarded osmosis: potential solutions for global challenges in energy and water supply. Chem. Soc. Rev. 42: 6959-6989, http://10.1039/C3CS60051C
[10] Rui Long, Xiaotian Lai, Zhichun Liu, Wei Liu. 2019. Pressure retarded osmosis: operating in a compromise between power density and energy efficiency. Energy, In press, accepted manuscript, Available online
[11] Rui Long, Xiaotian Lai, Zhichun Liu, Wei Liu. 2018. A continuous concentration gradient flow electrical energy storage system based on reverse osmosis and pressure retarded osmosis. Energy, Volume 152, 1, p.p 896-905.
[12] Xiaotian Lai, Rui Long, Zhichun Liu, Wei Liu. 2018. Stirling engine powered reverse osmosis for brackish water desalination to utilize moderate temperature heat. Energy, Volume 165, Part A, 15, p.p 916-930
[13] Helfer F., Lemckert C., Anissimov Y.G. 2014. Osmotic power with Pressure Retarded Osmosis: Theory, performance and trends. A review. Journal of Membrane Science. 453: 337-358. https://doi:10.1016/j.memsci.2013.10.053.
[14] McGinnis RL, McCutcheon JR, Elimelech M. A novel ammonia-carbon dioxide osmotic heat engine for power generation. J. Membr. Sci 2007; 305: 13-19, https://doi.org/10.1016/j.memsci.2007.08.027
[15] Straub A.P, Deshmukh A, Elimelech M. 2015. Pressure-retarded osmosis for power generation from salinity gradients: is it viable?. Energy & Environmental Science, 9 (1).
[16] Handbook of Chemistry and Physics, 27th edition, Chemical Rubber Publishing Co., Cleveland, Ohio, 1943
[17] Planck M. Treatise on thermodynamics. 1917 2nd edn. Longmans Green & Co, London.
[18] Garcia AV, Thomsen K, Stenby EH. Prediction of Mineral Scale Formation in Geothermal and Oilfield Operations using the Extended UNIQUAC Model. Part I: Sulphate Scaling Minerals, (Geothermics, 34(2005)61-97) https://doi.org/10.1016/j.geothermics.2004.11.002
[19] Garcia AV, Thomsen K, Stenby EH. Prediction of Mineral Scale Formation in Geothermal and Oilfield operations using the Extended UNIQUAC Model. Part II: Carbonate Scaling Minerals, (Geothermics 35(2006)239-284) https://doi.org/10.1016/j.geothermics.2006.03.001
[20] Rodriguez JA, Ruiz JJ, Urieta JS. 2000. Termodinámica química. Síntesis. Volumen 5 de Ciencias Químicas. ISBN 84-7738-581-5.
[21] Linert W. Highlights in Solute-Solvent Interactions. Springer Science & Business Media, 11 dic. 2001.
[22] Mersmann A. Crystallization Technology Handbook. CRC Press, 8 may. 2001
[23] Magalhaes MCF, Konigsberger E, May PM, Hefter G. Heat Capacities of Concentrated Aqueous Solutions of Sodium Sulfate, Sodium Carbonate, and Sodium Hydroxide at 25^{o}C. J. Chem. Eng. Data 2002, 47, 590-598. https://doi.org/10.1021/je010314h CCC
[24] Bhatnagar ON, Campbel AN. Experimental data from Bhatnagar and Campbell, Osmotic Coefficients of Sodium Sulphate in water from 50 to 150^{o}C, Canadian journal of chemistry 59(1981)123-126. https://doi.org/10.1139/v81-019
[25] Gibbard H. F. Jr., Scatchard, G., Rousseau, R. A., and Creek, J. L. 1974. Liquid-vapor equilibrium of aqueous sodium chloride, from 298 to 373K and from 1 to 6 mol kg-1, and related properties. J. Chem. Eng. Data 19, 281-288
[26] Rard, J. A., Clegg, S. L. and Palmer, D. A. 2000. Isopiestic determination of the osmotic coefficients of Na_2SO_4(aq) at 25 and 50 ^{o}C, and representation with ion-interaction (Pitzer) and mole fraction thermodynamic models. J. Solution Chem. 29, 1-48.
[27] Pitzer K.S., 1993. Molecular Structure and Statistical Thermodynamics. Selected Papers of Kenneth S Pitzer. Pages: 536 World Scientific Publishing Co Pte Ltd, Singapore, Singapore, ISBN 10 9810214391
[28] Baker R.W. Membrane Technology and Applications. J. Wiley, new York, 2nd, 2004

[29] Ihsanullah, 2019. Carbon nanotube membranes for water purification: developments, challenges, and prospects for the future. Separation and Purification Technology, 209, p.p. 307-337